Society For Biomaterials

Matrices based on lineal and star fumarate-metha/acrylate copolymers for bone tissue engineering: Characterization and biocompatibility studies

M. Leticia Bravi Costantino,[1] Tamara G Oberti,[1] Ana M. Cortizo,[2] M. Susana Cortizo[1]

[1]Instituto de Investigaciones Fisicoquímicas Teóricas y Aplicadas (INIFTA), Facultad de Ciencias Exactas, Universidad Nacional de La Plata - CONICET CCT-La Plata, CC 16 Sucursal 4, 1900, La Plata, Argentina
[2]Laboratorio de Investigaciones en Osteopatías y Metabolismo Mineral (LIOMM), Departamento de Cs. Biológicas, Facultad de Cs. Exactas, UNLP, La Plata, Argentina

Received 19 July 2018; revised 18 September 2018; accepted 18 September 2018
Published online 25 October 2018 in Wiley Online Library (wileyonlinelibrary.com). DOI: 10.1002/jbm.a.36554

Abstract: This article presents the preparation of matrices from two new families of fumaric copolymers and the effect of structural differences on their physicochemical and biological behavior. Diisopropyl fumarate (DIPF) and poly(ethylene glycol) methyl ether methacrylate (OEGMA) or *N*-isopropylacrylamide (NIPAM) were copolymerized by conventional radical and RAFT polymerization to obtain lineal or start architectures, respectively. These copolymers were characterized by spectroscopic (FTIR and ^{1}H-NMR) and chromatographic methods. The thermal stability was studied by thermal gravimetric analysis, showing some differences in relation to the architecture and chemical nature of copolymers. SEM morphological analysis demonstrated that the surface of the matrices derived from OEGMA exhibited an irregular and rough surface, while DIPF–NIPAM copolymers presented smooth surface with nearly no significant porosity. The matrix obtained of both kinds of copolymers presented no cytotoxicity as it was evaluated using a model of macrophages on culture. Moreover, cell growth was better on the surfaces of the DIPF–NIPAM matrices, suggesting a good interaction with this matrix and its potential application as matrices for tissue engineering. © 2018 Wiley Periodicals, Inc. J Biomed Mater Res Part A: 107A: 195–203, 2019.

Key Words: fumaric copolymer, RAFT polymerization, thermal properties, cytotoxicity, biocompatibility

How to cite this article: Bravi Costantino ML, Oberti TG, Cortizo AM, Cortizo MS. 2019. Matrices based on lineal and star fumarate-metha/acrylate copolymers for bone tissue engineering: Characterization and biocompatibility studies. J Biomed Mater Res Part A 2019:107A:195–203.

INTRODUCTION

Functional copolymers could be defined as polymers incorporating into their structure functional groups give them particular properties that make them useful for specific applications. Thus, unsaturated conjugates aliphatic or aromatic structures, monomers carrying acidic, basic, zwitterionic or photosensible chemical groups, and hydrophobic–hydrophilic block combination are responsible for transporting electrons in polymer semiconductors, stimuli-responsive polymers, or antifouling and self-assembly structures of predictable size for different applications, respectively.[1–4]

Dialkyl fumarates (DRF) are 1,2-disubstituted ethylenic monomers whose homo-polymerization behavior is characterized by a slow kinetics of reaction due to a significant steric hindrance during the propagation step.[5] However, DRF with bulky substituents (isopropyl, tert-butyl, or cyclohexyl groups) has high polymerization reactivity because of the decrease in bimolecular termination rate between polymer radicals bearing bulky substituents.[6,7] In contrast, radical copolymerization of DRF with electron-donating monomers readily proceed; diisopropyl fumarate (DIPF) and styrene or vinyl acetate produce copolymers with high tendency to the alternation.[8] On the other hand, dialkyl fumarates show low reactivity toward electron-accepting monomers, such as acrylates, methacrylates, or acrylonitrile. Despite their low reactivity, some DRF-metha/acrylate copolymers have been synthesized not only to clarify the monomer structure reactivity and the polymer structure–property relationship of these monomers but also for the potential applications that derive from them.[9–11]

Very few examples of amphiphilic fumaric copolymers appear in the literature. Berlinova et al. synthesized isopropyl pentachlorophenylfumarate (PCPFA) and isopropyl succinimido fumarate (SIFA), which were copolymerized with styrene (St) or *N*-vinyl pyrrolidone (VP).[12] Later, these copolymers were transformed in amphiphilic graft

Correspondence to: M. Susana Cortizo; e-mail: gcortizo@inifta.unlp.edu.ar
Contract grant sponsor: Facultad de Ciencias Exactas, Universidad Nacional de La Plata; contract grant number: 11/X768
Contract grant sponsor: Agencia Nacional de Promoción Científica y Tecnológica (ANPCYT); contract grant number: PICT-2015-0913
Contract grant sponsor: Consejo Nacional de Investigaciones Científicas y Técnicas (CONICET); contract grant number: PIP-D0047
Contract grant sponsor: Comisión de Investigaciones Científicas de la Provincia de Buenos Aires (CICPBA)

copolymers by introduction of amino-functionalized methoxypoly(oxyethylene) group. These copolymers presented a partially crystalline structure and good capacity to form stable emulsions. Alternating copolymers of *p*-10-undecenoyl-oxyphenyldimethylsulfonium methylsulfate (UPDS) and DRFs with relatively high molecular weights were obtained by Takahashi and coll.[13] The UPDS monomer behaves as polymerizable surfactants and its reactivity in different solvents, as well as its thermal properties, were studied.

For several years, we have been studying the potential applications of fumaric homo- and copolymers in regenerative medicine, due to their interesting properties. These polymers are characterized by high thermal stability, solubility in common solvents of varied polarity, glass transition temperature (T_g) values that can be regulated by the appropriated selection of comonomers and amorphous and transparent solid structure with high tensile strength. These characteristics have allowed us to design films, porous, or nanostructured matrices.[14–17] In addition, we demonstrated that these matrices were able to support osteoblastic and chondroblastic growth and were biodegradable by cellular mechanisms, showing no evidence of cytotoxicity. Thus, our previous results have proved that these biomaterials have the suitable properties for bone or osteochondrogenic tissue engineering applications.

In this work, we synthesized two families of functional fumaric copolymers starting from diisopropyl fumarate (DIPF) and poly(ethylene glycol) methyl ether methacrylate (OEGMA) or *N*-isopropylacrylamide (NIPAM). We are interested in amphiphilic copolymers with adequate properties for potential biomedical applications.[15,17] It is also our interest to analyze the effect of the macromolecular architecture on their thermal behavior (related to the processability conditions of the materials) and on their biocompatibility. To carry out this investigation we use two methodologies of synthesis: conventional radical copolymerization which allows us to obtain lineal copolymers and reversible addition-fragmentation chain transfer (RAFT) polymerization using a tetra-functional chain transfer agent (CTA) to obtain start architecture. The effect of the architecture and the chemical structure of the copolymers on their thermal stability and surface morphologies are evinced through TGA analysis and scanning electron microscopy (SEM). In addition, we investigate the cytotoxicity and biocompatibility of these materials. Thus, it is possible to investigate the effect of the macromolecular architecture on the copolymer properties which are closely related to their applications.

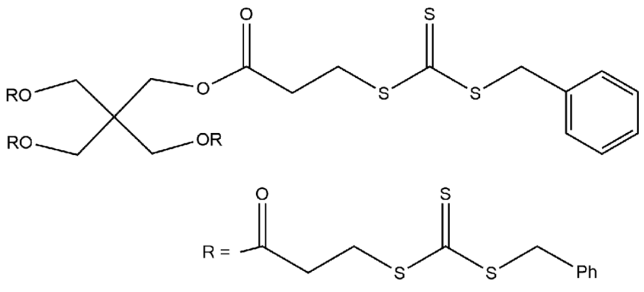

SCHEME 1. Molecular structure of the CTA used for the RAFT polymerization.

EXPERIMENTAL

Materials

Diisopropyl fumarate (DIPF) monomer was prepared and purified as previously described.[18] Briefly, fumaric acid (Biopack, Pure) and isopropanol (Sintorgan) were added to toluene (Ciccarelli), in the ratio 1:2.65 together with a catalytic amount of sulfuric acid (Merck, 95–97%) and the mixture was refluxed for 22 h. The product was purified by distillation under vacuum (yield 76%). Poly(ethylene glycol) methyl ether methacrylate (OEGMA), average M_n 500 was purchased from Sigma-Aldrich (Buenos Aires, Argentina) and was purified by filtration through basic alumina prior to use. *N*-isopropylacrylamide (NIPAM, 97%) was purchased from Sigma-Aldrich (Buenos Aires, Argentina), which was recrystallized from hexane. The chain transfer agent (CTA), pentaerythritoltetrakis (3-(S-benzyltrithio-carbonyl)propionate), (1) was synthesized following the previously published procedure.[19] Briefly, triethylamine (Sigma-Aldrich), pentaerythritol (Sigma-Aldrich), and carbon disulfide (Baker) were added in a flask at room temperature. After 1 h reaction, benzyl chloride (Sigma-Aldrich) was added dropwise. The reaction was carried out during 2 h. Finally, the product was purified by column chromatography using ethyl acetate: petroleum ether (30:70 v/v) (yield 50%). 2,2′-Azobisisobutyronitrile (AIBN) and benzoyl peroxide (BP) were purchased from Sigma-Aldrich (Buenos Aires, Argentina) and used after recrystallization from methanol. Toluene, hexane, chloroform, and other solvents were purchased from Cicarelli and Anedra (PA) (Buenos Aires, Argentina).

Copolymer synthesis

Radical copolymerization of DIPF with OEGMA or NIPAM (FO_L and FN_L, respectively) was carried out in solution of toluene (25% v/v) under microwave energy or thermal heating at 60°C, respectively, following a published procedure.[20] In the first case, DIFP and OEGMA (75:25) together with the solvent and the previously weighed mass of the initiator (AIBN, 40 mM) were charged into a conical Pyrex flask of 25 mL, and then purged with N_2 during 30 min. Then the reaction vessel was irradiated at 140 W for 15 min using a microwave oven (Zenith, ZVP-2819). In the second case, DIPF and NIPAM (75:25) copolymerization was carried out introducing both monomers and the solvent into a reaction tube with a preweighed amount of initiator (AIBN, 40 mM). The mixtures were degassed by three freeze–pump–thaw cycles in a vacuum line system, then sealed and immersed into a thermostat at 60°C. The reaction times were 2 or 4 days in the absence of light, for the conventional or RAFT radical copolymerization, respectively.

RAFT copolymerization was carried out with the same monomers composition (FO_S and FN_S), including a CTA as component of initiator system, using the following molar

relationship: [M]/[CTA]/[AIBN]: 3042/2.3/1; here [M] represent the total monomer molar concentration.

After reaching room temperature, the copolymers were isolated by hexane addition and purified twice by solubilization–precipitation (chloroform: hexane, 1:10). Finally, the copolymers were dried at constant weight for conversion (%C) estimation by gravimetry.

Copolymer characterization

^{1}H NMR spectra of polymers were recorded with a Variam-200 MHz (Mercury 200) at 35°C in $CDCl_3$. Tetramethylsilane (TMS) was used as an internal standard.

Fourier transform infrared spectra (FTIR) of the copolymer films deposited onto a sodium chloride (NaCl) window were recorded on a Nicolet 380 FTIR (Thermo Electron Corporation, Madison, WI) between 4000 to 400 cm^{-1} with a resolution of 4 cm^{-1} and 32 accumulated scans. The EZOMNIC software (EZOMNIC 7.4.127, Thermo Fisher Scientific Inc., Madison, WI) was used to analyze the spectra.

The molecular weight distribution and the average molecular weights were determined by size exclusion chromatography (SEC), using a LKB-2249 instrument at 25°C. A series of four μ-Styragel® columns—ranging in pore size 10^5, 10^4, 10^3, and 100 Å—was used with chloroform as an eluent. The sample concentration was 4–5 mg/mL and the flow rate was 0.5 mL/min. The polymer was detected by the carbonylic absorption of the ester group (5.75 μm), using an infrared detector (Miram 1A Infrared Analyzer) and the calibration was done with poly(methyl methacrylate) (PMMA) standards supplied by Polymer Laboratories and Polysciences.

Thermogravimetric analysis

Thermogravimetric analysis (TGA) was performed in a TGA-51 Shimadzu thermogravimetric analyzer. The temperature range was 20°C–600°C, at 10°C min^{-1} heating rate, 40 mL/min nitrogen flux, and 2–7 mg mass sample.

Preparation of the matrices and characterization

To perform experiments with macrophage cells in culture, matrices of copolymers were obtained by the solvent casting methodology. Polymer solutions were prepared in chloroform (5% wt/wt) and the solvent evaporated at room temperature in Teflon molds. Then the resulting films were dried under vacuum until constant weight. The films were sterilized by UV exposition for 2 h.[21] The surfaces of the matrices were coated with gold and their morphology was examined using scanning electron microscopy (SEM, Philips 505), with an accelerating voltage of 20 kV. The images were analyzed by Soft Imaging System ADDAII.

RAW264.7 macrophages culture, incubations, biocompatibility, and cytotoxicity studies

Murine macrophage RAW 264.7 cells were grown in DMEM (Invitrogen, Buenos Aires, Argentina) containing 10% fetal bovine serum (FBS, Natacor, Argentina), 100 U/mL penicillin and 100 mg/mL streptomycin at 37°C in a 5% CO_2 atmosphere. For the experiments, polymeric films were cut to size, inserted in a 24-well plate and macrophages plated on them.

The influence of the different materials on cell growth was tested using the counting of cells after 24 h of cultures on different films. For this purpose, after the culture period, cells were washed with PBS, fixed with methanol, and stained with Giemsa as we have previously described.[22] Cells per field were counted and the morphology of RAW264.7 cells cultured on the tissue culture polystyrene (TCPS) control wells and matrices was analyzed using a TS100 Eclipse Nikon microscope and photographed with a CCD camera with a 0.7× DXM Nikon lens. In addition, matrices were seeded with macrophages for 24 h and analyzed for SEM. For that purpose, matrices were fixed with 96% ethanol for 10 min at room temperature. After that, samples were dehydrated with graded ethanol series and finally dried at room temperature and coated with gold. The samples were analyzed as described for matrix alone.

Likewise, the cytotoxicity was evaluated by the measurement of nitric oxide (NO) in the culture media.[15] RAW 264.7 cells were grown on matrices or tissue culture plate (control condition), without or with 1 μg/mL LPS (positive control of cytotoxicity), was cultured using 1% FBS-DMEM medium without phenol red in a humidified atmosphere of 95% air and 5% CO_2 and incubated for 24 h. After this culture period, the medium was salved to evaluate for NO production by the Griess' assay. Cells were fixed with methanol for 5 min and stained with Giemsa for 10 min. After the films and monolayer were washed with top water, they were photographed using a Nikon microscope with a 40× objective lens. Cells were counted using the Imagen J program and results expressed as the number of cells/field.

Statistical analysis

Student's *t* test was used for comparisons between the control and experimental groups. All results are expressed as mean ± SEM and represent at least three different experiments performed in triplicate.

RESULTS

Copolymers synthesis and characterization

Copolymers of DIPF and OEGMA (FO) were synthesized by conventional radical and RAFT polymerization to obtain lineal (FO_L) or start architectures (FO_S), respectively. Figure 1A shows the structure of the copolymers confirmed by FTIR and ^{1}H-NMR spectra. FTIR (thin film, FO_L): (cm^{-1}), 2942, 2872 (C–H), 1730 (C═O), 1250, 1100 (CO–OR), 1110 (C–O). In addition, FO_S presented characteristic bands of aromatic and thioesters groups (cm^{-1}): 1600 (C═C, Ar), 748, 706 (C–H, Ar), 858 (C–S), 1293 (C═S), which can be assigned to the CTA structure. Figure 2A shows the NMR spectrum of FO_L, ^{1}H-NMR (DCl_3C, δ_η, ppm): 0.86 (CH–(C**H**$_3$)$_2$); 1.03 (–C–C**H**$_3$); 1.27 (–C**H**$_2$– main chain); 1.88 (–C**H**< main chain); 3.39 (–O–C**H**$_3$); 3.50–3.65 (–O–C**H**$_2$–C**H**$_2$–O–); 4.09 (–CO–O–C**H**$_2$–); 4.97 (–C**H**–(CH$_3$)$_2$), confirming the corresponding structure. FO_S ^{1}H-NMR spectrum (data not shown) presented other less relevant signals belonging to CTA structure: 2.75 (–CO–C**H**$_2$–); 3.28 (–C**H**$_2$–S–); 3.40(C–C**H**$_2$–O–); 6.80 (C**H** aromatic).

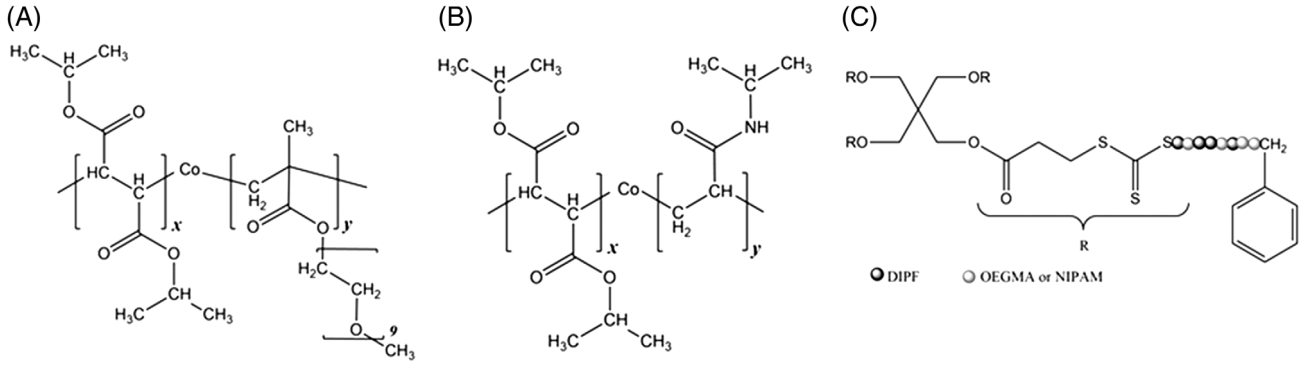

FIGURE 1. Structure of synthesized copolymers: FO (A), FN (B), and the schematic representation of the RAFT-copolymers of four branched star architecture (C).

Copolymers of DIPF and NIPAM were synthesized similarly with lineal (FN_L) or star architecture (FN_S) and their structure is presented in Figure 1B. FTIR (thin film, FN_L): (cm^{-1}), 3432 (N–H), 2982, 2930 (C–H), 1729 (C═O ester), 1644 (C═O amide), 1230, 1167 (CO–OR), 1108 (C–O). Figure 2B shows the NMR spectrum of FN_L, ^{1}H-NMR (DCl_3C, δ_η, ppm): 1.22 ((CH_3)$_2$); 1.81 (–C**H**$_2$– main chain); 2.08 (–C**H**< main chain); 4.01 (–NC**H**<); 4.96 (–C**H**–(CH_3)$_2$), confirming the corresponding structure. FN_S ^{1}H-NMR spectrum (data not shown) presented other less relevant signals belonging to CTA structure: 2.77 (–CO–C**H**$_2$–); 3.42 (–C**H**$_2$–S–); 6.80 (CH aromatic).

The composition of star and linear FO copolymers was estimated from the integral ratio of the peaks at 4.97 and 3.39 ppm corresponding to (–OC**H<**) of DIPF and (–OC**H**$_3$) of OEGMA, respectively, using Eq. 1.

$$F_1 = \frac{3\,\mathrm{I(OCH)}}{3\mathrm{I(OCH)} + 2\mathrm{I(OCH_3)}} \quad (1)$$

where F_1 is the mole fraction of DIPF in the copolymer and I(OCH) and I(OCH_3) represent the ^{1}H-NMR resonance peak areas at 4.97 and 3.39 ppm, respectively.

The composition of star and linear FN copolymers was estimated from the integral ratio of peaks at 4.96 and 4.02 corresponding to (–OC**H<**) of DIPF and (–NC**H**<) of NIPAM, respectively, using Eq. 2.

$$F_1 = \frac{I(\mathrm{OCH})}{I(\mathrm{OCH}) + 2I(\mathrm{NCH})} \quad (2)$$

where F_1 is the mole fraction of DIPF in the copolymer and I (OCH) and I(NCH) represent the ^{1}H-NMR resonance peak areas at 4.93 and 4.02 ppm, respectively.

Table I summarizes the mole fraction of DIPF in the feed (f_1), in the copolymer (F_1), percentage of reaction conversion (%C), and properties of the copolymers obtained. For the FO system was observed that the reaction conversion of conventional radical copolymerization (at the same reaction time) is higher than RAFT conditions, as it was expected according to the different polymerization mechanisms.[19] In both cases, the DIPF copolymer composition (F_1) was low, in spite of the high initial composition (f_1), suggesting that this monomer is consumed much more slowly than OEGMA during the copolymerization reaction. The average molecular weights (M_w) of the copolymers were similar in their magnitude but

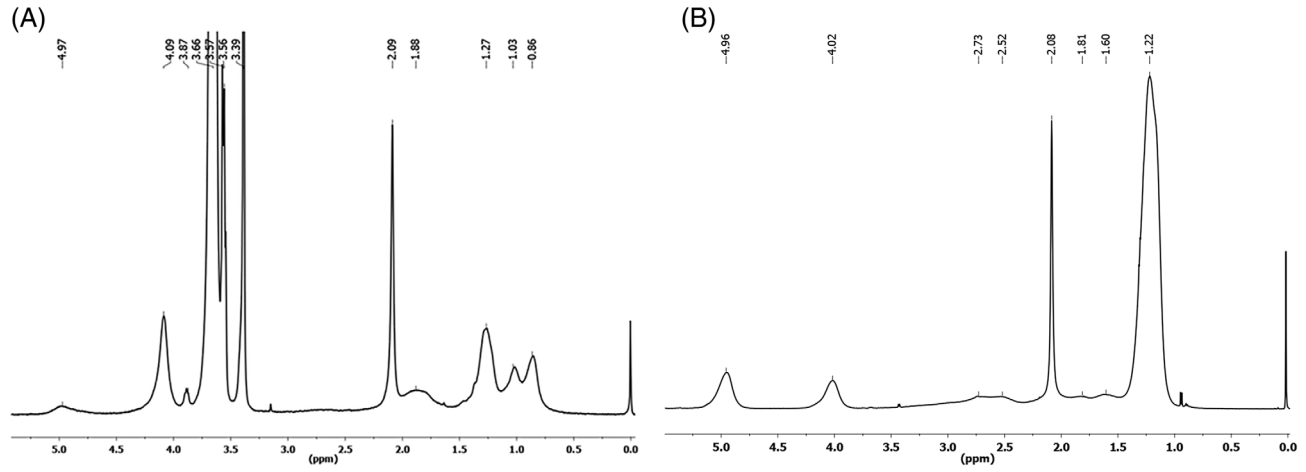

FIGURE 2. ^{1}H-NMR spectrum of each copolymer: FO (A) and FN (B).

TABLE I. Characteristics of the Synthesized Copolymers

Sample	*Initiator*	*Condition*	*Time h*	f_1[a]	F_1	*%C*	M_w (kg/mol)	PDI
FO_L	AIBN	MW	0.25	75	13	39	113.5	8.0
FO_S	CTA/AIBN	MW	0.25	75	6	14	154.5	4.2
FN_L	AIBN	Thermal	48	75	39	30	486.0	7.0
FN_S	CTA/AIBN	Thermal	96	75	36	22	17.2	2.9

Microwave condition (MW): 140 W; thermal condition: 60°C. [M]/[CTA]/[AIBN]: 3042/2.3/1 for RAFT polymerization or [AIBN] = 40 mM for conventional radical copolymerization.
[a]DIPF feed composition.

with high polydispersity, although somewhat lower under RAFT conditions.

The FN copolymers exhibited a different behavior; under similar reaction conversion, the DIPF composition in the copolymer was close to 40 in both cases suggesting that the preference of the growing macroradical toward the DIPF monomer is higher than in the FO system. On the other hand, the M_w of the copolymers prepared under RAFT conditions were one order of magnitude lower than under conventional conditions, but with better control of the reaction, which was evident for the lowest PDI. For both types of copolymers (FO and FN), the conventional radical polymerization seems to be faster than the RAFT polymerization when they are compared in reaction rate (2.6%, 0.93%, 0.01%, and 0.004%/min for FO_L, FO_S, FN_L, and FN_S, respectively).

Thermal properties

The thermal stability analysis of copolymers with different architecture was assessed by TGA under nitrogen atmosphere; their decomposition curves are depicted in Figure 3A,B. FO copolymers seemed to decompose in a two-stage process and showed higher initial decomposition temperatures (IDT, Table II) than PDIPF and POEGMA homopolymers. The onset degradation temperature for PDIPF and POEGMA, to be 250°C and 210°C, respectively.[20,23] The first step of decomposition could be ascribed to the PEG's side chains lost, as it was observed for other structurally related copolymers.[24] The last major decomposition step with a higher experimental loss of mass, at a maximum temperature value of 373°C for linear polymers (FO_L) and 338°C for branched polymers (FO_S), could be attributed to the random main chain scission.

Similarly, the FN copolymers exhibited a two-stage thermal decomposition [Fig. 3(B)] with an intermediate IDT at the IDT of the corresponding homopolymers; 250°C and 350°C for PDIPF and PNIPAM, respectively.[25] The thermogram of FN_S shows a first degradation event up to 150°C, which could correspond to residual solvents or environment water adsorbed. No significant differences were observed between the maximum decomposition temperatures (T_{max1} and T_{max2}) of both copolymers (FN_S and FN_L).

Matrix characterization

The morphological characteristics of matrices prepared from FO and FN copolymers were analyzed through SEM images (Fig. 4). As can be seen in Figure 4A,B, FO matrices exhibited an irregular and rough surface. In contrast, FN matrices presented smooth surface with nearly no significant porosity [Fig. 4(C,D)]. In both cases, very small differences were observed in relation to the architecture of the copolymers, being the surface of the matrices from linear copolymers somewhat rougher.

Biocompatibility and cytotoxicity study

The growth and possible cytotoxicity of the films were evaluated using the cell morphology, cell number counting, and NO production of raw macrophages growing on different films or standard tissue culture plates as control. Cells growing on TCPS [Fig. 5(A)] showed a round aspect with few extensions and a well-stained central nucleus. As we have

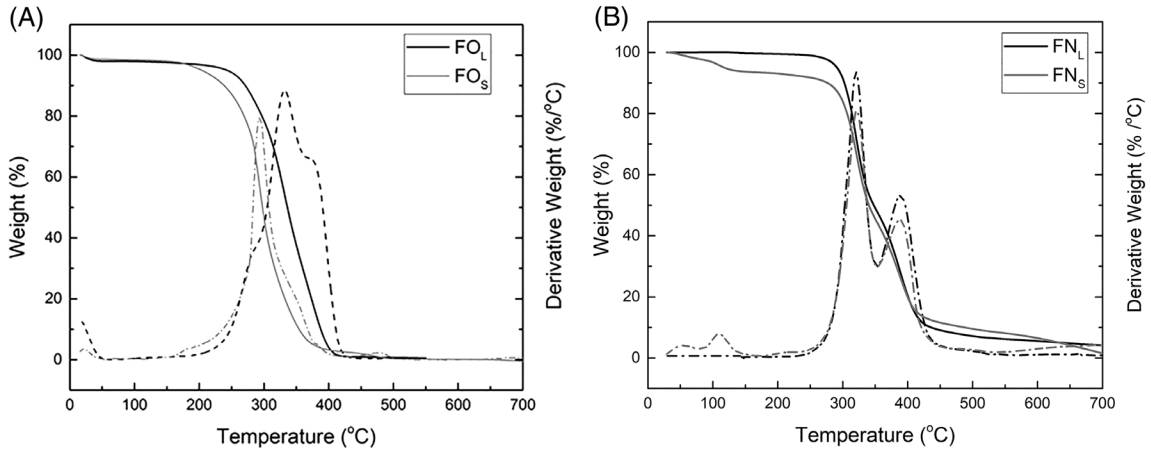

FIGURE 3. (A) TGA (—) and DTG (---) curves for FO_L (black) and FO_S (gray); (B) TGA (—) and DTG (---) for FN_L (black) and FN_S (gray).

TABLE II. TGA Data of Fumaric Copolymers

Sample	F_1	IDT	T_{max1} [a]	T_{max2} [a]
FO_L	13	271	332 (13)	373(34)
FO_S	8	238	293 (22)	338 (74)
FN_L	39	267	320 (27)	388 (71.5)
FN_S	36	244	321.5 (34)	388.5 (73.5)

[a]Value in parentheses indicates the percentage of total mass lost (%) up to the stated temperature (°C).

previously reported, when these cells are exposed to lipopolysaccharide (LPS) as a positive control of cytotoxicity, they show a cytoplasm with several extensions, suggesting activation of the macrophages.[15] In the presence of LPS, a clear cytotoxic effect was observed, cells shown a stellated aspect, shrinkage, and several cytoplasm extensions [Fig. 5(B)]. Cells growing on FO films showed a round or fibroblastic in form with one or two extensions, although small numbers of cells seem to proliferate on this kind of matrix. Not many differences were observed between FO_L [Fig. 5(C)] and FOs [Fig. 5(D)] films; beside, on the last one, cells grew mainly in clams instead of in an isolated way. On the other hand, cells on FN_L film [Fig. 5(E)] showed a round aspect similarly to the control monolayer, with few extension and no signs of cytotoxicity. In addition, macrophages on FNs film [Fig. 5(F)] also showed a normal aspect, although they seem to be more rounded with no cellular processes.

Table III shows that the NO production was similar when cells had been grown on TCPS control wells or into either of the different films. In addition, cells respond to the toxic agent LPS by increasing the NO production into the conditioned media after 24 h of culture.

In addition, we observed the morphology of raw macrophages growing on the surfaces of start matrices of FO or FN by SEM (Fig. 6). No differences were observed in relation to the architecture of the starting copolymers (data no shown). It can be seen that cells grew on the matrix and interacted with them, although more cells appeared on the FNs films.

DISCUSSION

In previous studies, we demonstrated that homo- and copolymerization of DIPF under microwave energy exhibited a significant enhancement of the reaction rate in comparison with thermal polymerization conditions.[10,18,20] In this study, we prepared new amphiphilic copolymers starting to DIPF and OEGMA monomers using the same methodology. The results shown that the FO copolymer contains low proportion of DIPF monomer, in spite of the high initial composition of its comonomer. Under similar reaction conditions, FN copolymers showed a highest content of DIPF into the macrostructure, which indicates a greater reactivity of the propagating macroradical toward this comonomer. These results agree to the previously observed for other copolymerization reactions between dialkyl fumarates and acrylic or methacrylic monomers.[8–10]

The study of the thermal properties of polymers that are designated to use in medical applications is important given that they must be able to withstand processing and sterilization. The main methods for manufacturing medical devices,

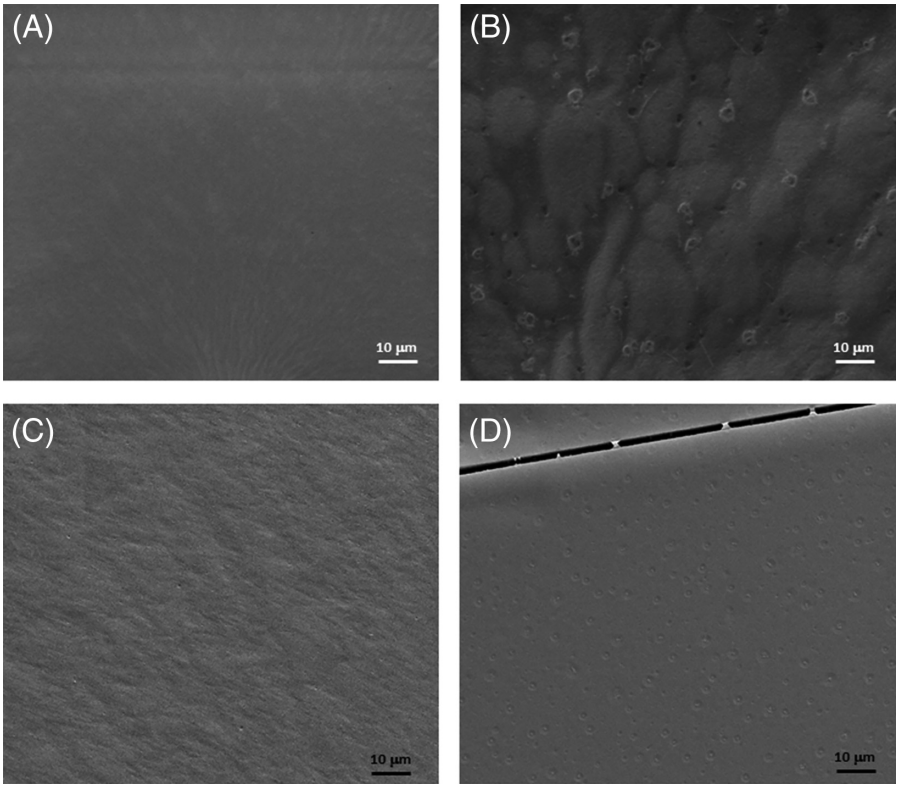

FIGURE 4. SEM images of surfaces of matrices prepared of copolymers: (A) FO_L, (B) FO_S, (C) FN_L, and (D) FN_S.

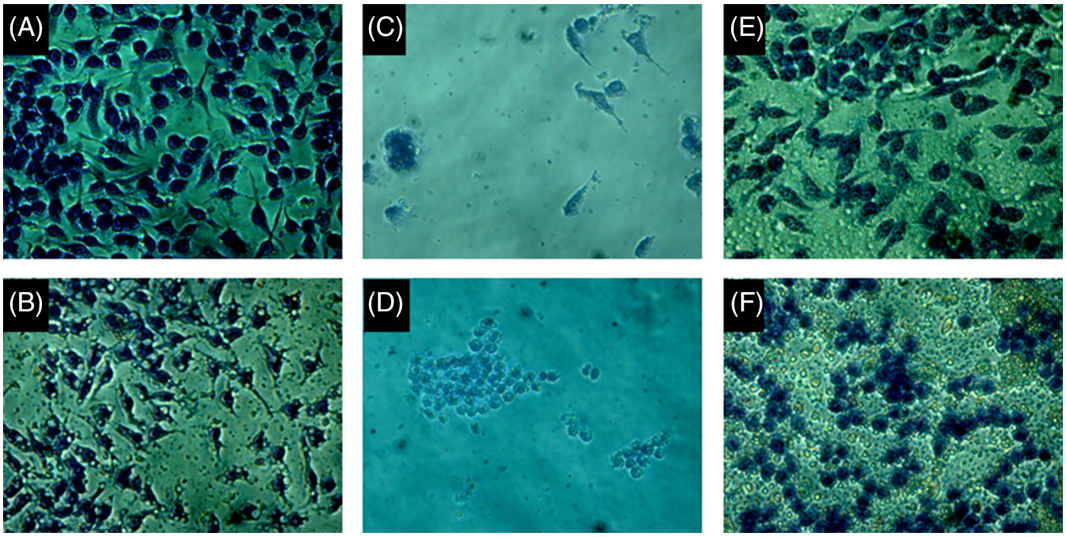

FIGURE 5. Raw macrophages were grown on 1% FBS-DMEM without phenol red on TCPS control (A), control plus 1 μg/mL LPS (B), FO_L (C), FO_S (D), FN_L (E), or FN_S film (F) during 24 h. Cells stained with Giemsa were photographed and counted. Objective lens: 40×.

TABLE III. NO Production and Proliferation Assay of Raw Macrophages Growing on TCPS Control or Fumaric Copolymers Matrices

Matrix	NO [nmol mL^{-1}]	Cell number/field
TCPS (control)	1.07 ± 0.08	123 ± 21
TCPS + LPS	4.23 ± 0.33	22 ± 3
FO_L film	0.81 ± 0.08	26 ± 3
FO_S film	1.16 ± 0.04	30 ± 7
FN_L film	1.03 ± 0.06	142 ± 11
FN_S film	0.95 ± 0.04	120 ± 9

Values are expressed as mean ± SEM (n = 6).

such as melt pressing, and commonly used sterilization techniques, are all heat- or moisture-related.[26] Also during these processing the materials should not form toxic or harmful products for the human body.[27] Thus, the thermal studies of FO and FN copolymers were carried out. The thermal stability of FO copolymers was different regarding its architecture. The lowest IDT and maximum decomposition temperatures (T_{max1} and T_{max2}) of FO_S in comparison to FO_L could be attributed to the weakness of thioester bonds that are present into the branched structure of this copolymer. These results suggest that the branched star copolymer is thermally less stable than the linear copolymer of the same chemical nature. On the other hand, FN copolymers did not shown differences in the thermal stability in relation to its architecture. In both cases (FN_S and FN_L), two thermal events were observed, the first of one could be attributed to the loss of the lateral group by cleavage reaction of the pendent group, as was previously demonstrated for other structurally related fumaric copolymers.[20] Previous studies on polyacrylamide and its copolymers with methyl methacrylate demonstrated that below 340°C, the main degradation products are ammonia and methanol which evolve through the cyclic imide formation.[28] In fact, in our work a similar degradation mechanism should be considered, due to a similar thermal degradation mechanism that was proved for poly(*N*-alkyl acrylamide).[25] Finally, at higher temperatures, the scission of the main chain will occur.

It is known that the chemical nature of the materials as much as the surface characteristic of the matrices can modify significantly the biomaterial–cell interaction, which is a key factor for the cell adhesion and proliferation process.[29,30] In our systems, the matrices did not show significant differences in relation to the architecture of the copolymers,

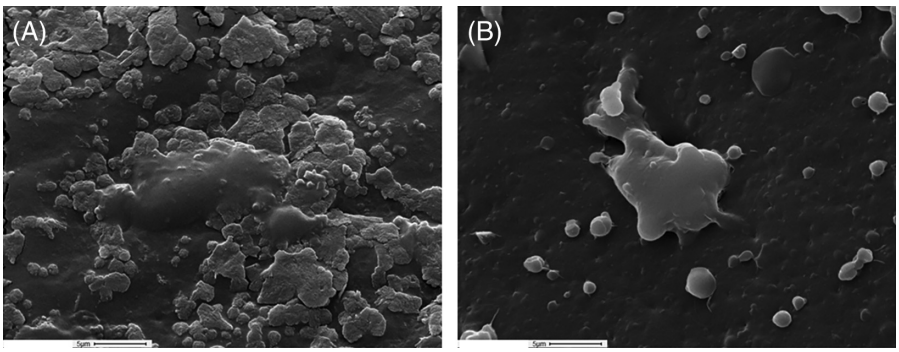

FIGURE 6. SEM image of raw macrophages growing on (A) FO_S or (B) FN_S surface of matrices.

suggesting that this macromolecular characteristic does not affect in an important way the superficial morphology.

Previously it has been shown that macrophages are a very sensitive culture model to evaluate possible *in vitro* inflammatory responses to a material with potential applications in tissue engineering.[22,31,32] The counting of cells that proliferate on films after 24 h agrees with the observation of cells by microscopy. Few cells proliferate on FO films, suggesting a poor interaction with these matrixes. On the other hand, when cells were plated into a FN films, cells attached and proliferated adequately, showing a good interaction with the matrices after 24 h of culture. No significant differences were observed in the NO production and cells number in relation to the architecture of the copolymers (start and linear structure), suggesting no cytotoxicity under the present conditions. The results suggest that the biocompatibility of macrophages with the different films could be attributed to the chemical nature of the copolymer but not to their macromolecular architecture.

CONCLUSIONS

Two families of functional fumaric copolymers were synthetized by conventional or RAFT radical polymerization to obtain linear or start architectures, respectively. These copolymers were identified and characterized by spectroscopic and chromatographic methods revealing their structural differences. The TGA analysis demonstrated that the branched star copolymer (FO_S) is thermally less stable than the linear copolymer (FO_L); while no significant differences were observed between the maximum decomposition temperatures of FN_S and FN_L. The surface morphological characteristics of matrices prepared from FO copolymers were more irregular and rough than those of FN copolymers, without significant differences in relation to the architecture of the polymer from which they derive. Finally, the biocompatibility and cytotoxicity studies revealed that none of the materials obtained exhibit cytotoxicity, although the raw macrophage cells grew better on the matrices prepared by casting the FN copolymers, indicating a better interaction of these cells with the surface of material.

ACKNOWLEDGMENTS

The authors thank Ms María Cecilia Moreno for the revision and improvement of the language of this article. LBC is a fellowship form CONICET; AMC is a member of Carrera del Investigador Cientifico (CICPBA); TGO and MSC are members of Carrera del Investigador Cientifico from CONICET.

REFERENCES

1. Choi J, Song H, Kim N, Kim FS. Development of n-type polymer semiconductors for organic field-effect transistors. Semicond Sci Technol 2015;30(6):16.
2. Rzaev ZMO, Dinçer S, Pişkin E. Functional copolymers of N-isopropylacrylamide for bioengineering applications. Prog Polym Sci 2007;32:534–595.
3. Zheng L, Sundaram HS, Wei Z, Li C, Yuan Z. Applications of zwitterionic polymers. React Funct Polym 2017;118:51–61.
4. Schacher FH, Rupar PA, Manners I. Functional block copolymers: Nanostructured materials with emerging applications. Angew Chem Int Ed 2012;51:2–25.
5. Otsu T, Ito O, Toyoda N, Mori S. Polymers from 1,2-disubstituted ethylenic monomers, 2. Homopolymers from dialkyl fumarates by radical initiator. Makromol Chem Rapid Commun 1981;2:725–728.
6. Yamada B, Yoshikawa E, Shiraishi K, Miura H, Otsu T. Determination of absolute rate constants for radical polymerization of diisopropyl fumarate based on a quantitative scavenge of propagating radical. Polymer 1991;32:1892–1896.
7. Matsumoto A, Sano Y, Yoshioka M, Otsu T. Radical polymerization of dicyclohexyl fumarate and its derivatives as studied by electron spin resonance spectroscopy. Eur Polym J 1996;32:1079–1085.
8. Otsu T, Matsumoto A, Shiraishi K, Amaya N, Koinuma Y. Effect of the substituents on radical copolymerization of dialkyl fumarates with some vinyl monomers. J Polym Sci Part A: Polym Chem 1992;30:1559–1565.
9. Baruah SD, Sarmah D, Laskar NC. Copolymers of bulky fumarate: Synthesis and their properties. J Polym Res 2011;18:225–233.
10. Oberti TG, Cortizo MS, Alessandrini JL. Novel copolymer of diisopropyl fumarate and benzyl acrylate synthesized under microwave energy and quasielastic light scattering measurements. J Macromol Sci Part A: Pure Appl Chem 2010;47:725–731.
11. Jansen JFGA, Houben EEJE, Tummers PHG, Wienke D, Hoffmann J. Real-time infrared determination of photoinitiated copolymerization reactivity ratios: Application of the Hilbert transform and critical evaluation of data analysis techniques. Macromolecules 2004;37:2275–2286.
12. Berlinova IV, Amzil A, Tsvetkova S, Panayotov IM. Amphiphilic graft copolymers with poly (oxyethylene) side chains: Synthesis via activated ester intermediates-properties. J Polym Sci Part A: Polym Chem 1994;32:1523–1530.
13. Takahashi K, Suzuki M, Kido J, Kuramoto N, Nagai K. Alternating copolymerization of a surface active monomer having an active ester group with dialkyl fumaratos. Polymer 1995;36:4675–4681.
14. Cortizo MS, Molinuevo MS, Cortizo AM. Biocompatibility and biodegradation of polyester and polyfumarate based-scaffolds for bone tissue engineeringJ. Tissue Eng Regen Med 2008;2:33–42.
15. Fernández JM, Cortizo MS, Cortizo AM. Fumarate/ceramic composite based scaffolds for tissue engineering: Evaluation of hydrophylicity, degradability, toxicity and biocompatibility. J Biomater Tissue Eng 2014;4:227–234.
16. Fernández JM, Cortizo MS, Cortizo AM, Abraham GA. Osteoblast behavior on novel porous polymeric scaffolds. J Biomater Tissue Eng 2011;1:1–7.
17. Lastra ML, Molinuevo MS, Cortizo AM, Cortizo MS. Fumarate copolymer – Chitosan crosslinked scaffold directed to osteochondrogenic tissue engineering. Macromol Biosci 2017;17:1600219.
18. Cortizo MS, Laurella S, Alessandrini JL. Microwave-assisted radical polymerization of dialkyl fumarates. Radiat Phys Chem 2007;76:1140–1146.
19. Mayadunne RTA, Jeffery J, Moad G, Rizzardo E. Living free radical polymerization with reversible addition-fragmentation chain transfer (RAFT polymerization): Approaches to star polymers. Macromolecules 2003;36:1505–1513.
20. Oberti TG, Alessandrini JL, Cortizo MS. Thermal characterization of novel p-nitrobenzylacrylate-diisopropyl fumarate copolymer synthesized under microwave energy. J Therm Anal Calorim 2012;109:1525–1531.
21. Fernández JM, Molinuevo MS, McCarthy AD, Cortizo AM, Cortizo MS. Characterization of poly(ε-caprolactone)/polyfumarate blends as scaffolds for bone tissue engineering. J Biomater Sci Polym Ed 2010;21:1297–1312.
22. Cortizo AM, Ruderman G, Correa G, Mogilner IG, Tolosa EJ. Effect of surface topography of collagen scaffolds on cytotoxicity and osteoblast differentiation. J Biomater Tissue Eng 2012;2:125–132.
23. Wang P, Tan KL, Kang ET, Neoh KG. Synthesis, characterization and anti-fouling properties of poly(ethylene glycol) grafted poly(vinylidene fluoride) copolymer membranes. J Mater Chem 2001;11:783–789.
24. Luzon M, Corrales T. Thermal studies and chromium removal efficiency of thermoresponsive hyperbranched copolymers based on PEG-methacrylates. J Therm Anal Calorim 2014;116:401–409.
25. Silva ME, Dutra ER, Mano V, Machado JC. Preparation and thermal study of polymers derived from acrylamide. Polym Degrad Stab 2000;67:491–495.
26. Odelius K, Plikk P, Albertsson AC. The influence of composition of porous copolyester scaffolds on reactions induced by irradiation sterilization. Biomaterials 2008;29:129–140.

27. Torabinejad B, Mohammadi-Rovshandeh J, Davachi SM, Zamanian A. Synthesis and characterization of nanocomposite scaffolds based on triblock copolymer of L-lactide, ε-caprolactone and nano-hydroxyapatite for bone tissue engineering. Mater Sci Eng C 2014;42:199–210.
28. Grassie N, McNeill IC, Samson JNR. The thermal degradation of polymethacrylamide and coplymers of methacrylamide and methyl methacrylamide. Eur Polym J 1978;14:931–937.
29. Lastra ML, Molinuevo MS, Giussi JM, Allegretti PE, Blaszczyk-Lezak I, Mijangos C, Cortizo MS. Tautomerizable β-ketonitrile copolymers for bone tissue engineering: Studies of biocompatibility and cytotoxicity. Mater Sci Eng C 2015;51:256–262.
30. Rizzi SC, Heath DJ, Coombes AG, Bock N, Textor M, Downes S. Biodegradable polymer/hydroxyapatite composites: Surface analysis and initial attachment of human osteoblasts. J Biomed Mater Res 2001;55:475–486.
31. Bixby J, Ray TD, Chan FKM. TNF, cell death and inflammation. Curr Med Chem Antiinflamm Antiallergy Agents 2005;4: 557–567.
32. Denlinger LC, Fisette PL, Garis KA, Kwon G, Vazquez-Torres A, Simon AD, Nguyen B, Proctor RA, Bertics PJ. Regulation of inducible nitric oxide synthase expression by macrophage purinoreceptors and calcium. J Biol Chem 1996;271:337–342.